

Benchmarking multiconfigurational Hartree by the exact wavefunction of two harmonically trapped bosons with contact interaction

Yeongjin Gwak,¹ Oleksandr V. Marchukov,² and Uwe R. Fischer¹

¹*Center for Theoretical Physics, Department of Physics and Astronomy, Seoul National University, 08826 Seoul, Korea*

²*School of Electrical Engineering, Faculty of Engineering, Tel Aviv University, 6997801, Tel Aviv, Israel*

(Dated: November 13, 2018)

We consider two bosons in a one-dimensional harmonic trap, interacting by a contact potential, and compare the exact solution of this problem to a self-consistent numerical solution by using the multiconfigurational time-dependent Hartree (MCTDH) method. We thereby benchmark the predictions of the MCTDH method, and the statement that it is numerically exact, with a few-body problem that has an analytical solution for the most commonly experimentally realized interaction potential in ultracold quantum gases. It is found that exact ground state energy and first order correlations are accurately reproduced by MCTDH up to the intermediate dimensionless coupling strengths corresponding to typical background scattering lengths of magnetically trapped ultracold dilute Bose gases. For larger couplings, established for example by (a combination of) Feshbach resonances and optical trapping, the MCTDH approach overestimates the depth of the trap-induced correlation dip of first order correlations in position space, and underestimates the fragmentation, defined as the average relative occupation of orbitals other than the energetically lowest one. We anticipate that qualitatively similar features in the correlation function may arise for larger particle numbers, paving the way for a quantitative assessment of the accuracy of MCTDH by experiments with ultracold atoms.

The MCTDH method is a powerful self-consistent numerical approach to the quantum dynamics of many interacting particles, and has been extensively used to predict correlation functions, cf., e.g., Refs. [1–4]. Initially used for the purpose of propagating wavepackets in physical chemistry, where it is by now routinely used [5], in the past decade it has increasingly been applied to describe the intricate many-body physics of ultracold dilute Bose gases, for example, in Refs. [6–17].

The present study is inspired by the ongoing debate on the convergence of MCTDH, see, e.g., Refs. [18–21]. These convergence issues arise because the MCTDH equations of motion become singular as soon as unoccupied orbitals occur during the real or imaginary time evolution. Hence some (nonunique) prescription of regularization is needed, see for example [22–25]. Furthermore, it is not clear whether MCTDH is more accurate in comparison to, e.g., the alternative approach of using the truncated Wigner method for either large or small number of particles N [20]. This stems from the fact that neither method, MCTDH nor truncated Wigner (see also, e.g., Ref. [26]) provides a *control parameter* for its accuracy to be assessed within given numerical resources. This should be compared with (number-conserving) Bogoliubov theory [27, 28], where this control parameter is some power of the inverse of the particle number, $1/N$. Rigorous results on the accuracy of retaining just a single orbital in the field operator expansion are available in the limit of particle number $N \rightarrow \infty$, provided the (formal) condition is met that the interaction coupling g decreases as $1/N$, and hence $g = g(N)$ tends to zero in that limit [29, 30]. These rigorous results are, in addition, limited to reproducing the Gross-Pitaevskii energy correctly, while higher-order correlations reveal deviations

from mean-field physics even in the large N limit keeping gN fixed cf., e.g., [12, 13].

Importantly, a direct experimental verification of the accuracy of MCTDH is lacking so far. We here aim at benchmarking MCTDH with the exactly solvable model most closely associated with current experiments on ultracold gases: A pair of bosons with repulsive contact interactions trapped in a single harmonic well. Because many-body correlations are strongest in one spatial dimension, we use to this end a one-dimensional (1D) variant of the originally 3D analytical solution [31–33]: For a pair of bosons in one spatial dimension, one expects deviations from (single-orbital) mean-field physics to be most significant. The present case is therefore an excellent testing ground for the accuracy of MCTDH. Beyond the weak coupling regime and upon approaching the Tonks-Girardeau “fermionized” limit [34–37], the *self-consistent* determination of the orbitals’ shape in a harmonic trap becomes increasingly important, as the usual periodic boundary conditions in a spatially homogeneous system cannot be applied. While it is well known that in 1D, the Lieb-Liniger solution [38] is exact for any N , extracting the relevant correlation functions is a challenging task [35]. In addition, the Lieb-Liniger solution is not available in a harmonic trap.

The analytically solvable $N = 2$ problem provides us with an exact statement on the shape of the orbitals and level occupation statistics. It can thus rigorously assess the accuracy of MCTDH, which determines these quantities for a large but finite number M of field operator modes. We provide below, for the first time with an *experimentally realizable* interaction potential, an accurate quantitative statement to which extent MCTDH is “numerically exact” [39], i.e., controllably reproduces for

$M \rightarrow \infty$ an exact solution of the Schrödinger equation [40, 41]. In addition, the strength of the contact interaction potential investigated is controllable over a large range via Feshbach resonances [42], facilitating experimental access to the validity domain of MCTDH.

Analytical solution. The Hamiltonian is

$$H = -\frac{\hbar^2}{2m}\Delta_{\vec{x}} + \frac{1}{2}m\omega^2\vec{x}^2 + g\delta(x_1 - x_2), \quad (1)$$

where $\vec{x} = (x_1, x_2)$ is the position vector of the atoms, m their mass, ω the frequency of the trapping potential, and g is the 1D interaction coupling constant. Below, we use $\hbar\omega$ as unit of energy, and $l = \sqrt{\hbar/m\omega}$ as length scale.

The solution of the Schrödinger equation can be found by the separation ansatz [31, 33]

$$\Psi(R, r) = \Psi_{\text{COM}}(R)\psi_{\text{rel}}(r), \quad (2)$$

where we introduced relative, $r = \frac{1}{\sqrt{2}}(x_1 - x_2)$ and center-of-mass (COM) $R = \frac{1}{\sqrt{2}}(x_1 + x_2)$ coordinates. Relative and COM wavefunctions are then given by

$$\begin{aligned} \Psi_{\text{COM}}(R) &\propto e^{-R^2/2}H_n(R), \\ \psi_{\text{rel}}(r) &\propto e^{-r^2/2}U(-\nu, \frac{1}{2}; r^2), \end{aligned} \quad (3)$$

where H_n is the Hermite polynomial of order n and $U(-a, b; x)$ is a confluent hypergeometric function [43]; we omitted the normalization constants. A new quantum number ν parametrizes the total energy of the system

$$E = 2\nu + n + 1, \quad (4)$$

where the g dependence of ν is found by solving [33]

$$\frac{\Gamma(-\nu + \frac{1}{2})}{\Gamma(-\nu)} = -\frac{g}{2\sqrt{2}}. \quad (5)$$

Clearly, the wavefunction in Eq. (2) describes the system we consider exactly. In the following, we compare ground state energy, single-particle density matrix and the shape of the orbitals, obtained by employing this exact solution with the results from MCTDH calculations, varying the coupling g and the number of orbitals M .

Using Eqs. (2)–(3), the single-particle density matrix $\rho^{(1)}(x, x') = \int \Psi^*(x, x_1)\Psi(x_1, x')dx_1$ of the ground state, which is obtained from $n = 0$ and $\nu = \nu_0$ with ν_0 being the minimal value of ν from solving Eq. (5), is given by

$$\begin{aligned} \rho^{(1)}(x, x') &\propto e^{-(x^2+x'^2)/2} \\ &\times \int dx_1 e^{-\frac{x_1^2}{2}} U\left(-\nu_0, \frac{1}{2}; \frac{(x-x_1)^2}{2}\right) \times (x \leftrightarrow x'). \end{aligned} \quad (6)$$

where the integral may be calculated numerically to in principle arbitrary accuracy.

The MCTDH method. The notion of self-consistency

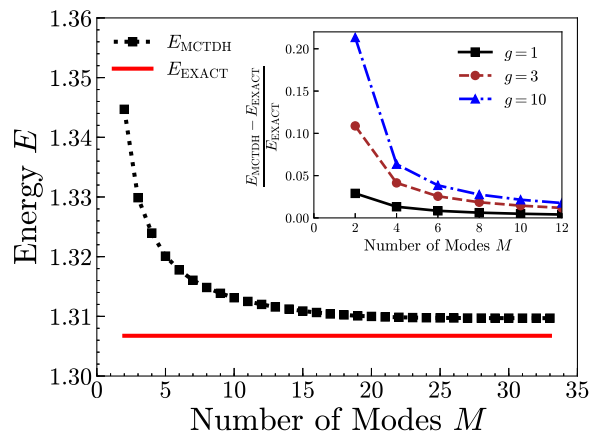


FIG. 1. Convergence of the ground state energy, calculated via MCTDH-X with increasing number of orbitals (black squares), $M = 2, \dots, 33$ towards the exact value from Eq. (4) (red solid); the coupling $g = 1$. Inset: The relative error for the ground state energy for $g = 1$ (black solid), $g = 3$ (brown dashed) and $g = 10$ (blue dash-dotted).

embodied by MCTDH is that it determines the shape and time dependence of the orbitals $\varphi_i(x, t)$ self-consistently together with their occupation distribution $C_{\vec{N}}(t)$ in Fock space, where $\vec{N} = (N_0, N_1, \dots, N_{M-1})$ ($\sum_0^{M-1} N_i = N$) is the occupation vector. The coupled MCTDH equations of motion are [33]

$$\begin{aligned} i\hbar \frac{\partial \mathbf{C}(t)}{\partial t} &= \mathbf{H}(t)\mathbf{C}(t), \\ i\hbar \frac{\partial |\varphi_j\rangle}{\partial t} &= \hat{P} \left[\hat{h}|\varphi_j\rangle + \sum_{k,s,q,l=1}^M \rho_{jk}^{-1} \rho_{ksql} \hat{W}_{sl} |\varphi_q\rangle \right]. \end{aligned} \quad (7)$$

Here, $\mathbf{C}(t)$ is the column vector that consists of all possible expansion coefficients $C_{\vec{N}}(t)$, $\mathbf{H}(t)$ corresponds to the time-dependent Hamiltonian matrix in the basis $|\vec{N}; t\rangle$, \hat{h} is the single-particle Hamiltonian, $\hat{W}_{sl} = g \int \int dx \varphi_s^*(x) \varphi_l(x)$, and $\hat{P} = 1 - \sum_{k'=1}^M |\varphi_{k'}\rangle \langle \varphi_{k'}|$ is an orthogonal subspace projection operator. Finally, ρ_{ksql} is the matrix element of the two-particle density matrix. To find the self-consistent solution of the above equations, we use MCTDH-X software package, provided by [4] and first implemented in [44, 45].

Convergence of MCTDH to exact ground state energy.

In order to verify convergence of the ground state energy to the exact result, we performed extensive MCTDH calculations for a wide range of the number of orbitals, $M = 2, \dots, 33$. In Fig. 1 we present the comparison between the exact and numerical values of the ground state energy for the interaction coupling $g = 1$. We conclude that the numerical value converges rapidly for a large number of orbitals. The relative error between the exact and converged numerical values becomes less than 3% when $M > 15$. We however also notice that upon

further increase of M , the error does not decrease significantly further. Specifically, for $M = 20$ the error is 2.48%, and for $M = 33$ it is still 2.26%. To illustrate the dependence of the convergence on g , the relative error for the energy, $(E_{\text{MCTDH}} - E_{\text{exact}})/E_{\text{exact}}$, is shown in the inset of Fig. 1 for $M = 2, \dots, 12$ and $g = 1, 3$, and 10. The MCTDH calculations still converge reasonably well for sufficiently large M to the exact energy. However, the computational cost (the M needed for convergence) is, as expected, seen to increase for larger values of g .

Density matrix. Generally, correlation functions are more sensitive to the accuracy of MCTDH predictions than the ground state energy is, cf. [12, 13, 46]. Therefore, we now concentrate on a comparison of the analytics to numerics in the form of the first-order correlations, as encapsulated by the single-particle density matrix. We compare the results of our MCTDH calculations, in addition, with the Monte Carlo calculations performed by Minguzzi *et al.* in Ref. [34] for the single-particle density matrix of a pair of hard-core bosons in a 1D harmonic trap [47]. The emphasis for this part of the paper is to assess the accuracy of MCTDH when g in the Hamiltonian Eq. (1) is varied from weak over intermediate to strong coupling, so that we here fix $M = 10$.

In Fig. 2, we plot the normalized single-particle density matrix $\rho^{(1)}(x, x')/\sqrt{\rho(x)\rho(x')}$ as function of x , and at fixed $x' = 0$, for relatively large values of g . The gray circles in the top panel are taken from the Monte Carlo data of Ref. [34], while the solid lines show the comparison of MCTDH results with the 1D variant of the 3D analytical solution for $N = 2$ bosons in a harmonic trap [31, 32]. We observe that the qualitative behavior of the MCTDH results is in accord with the analytical result as well as with the hard-core Monte Carlo calculations – the dip in the first-order correlations located at approximately $x = l$ is consistently visible. Note that this dip in the correlation function $\rho^{(1)}(x, x')$ corresponds to a peak in *phase fluctuations*, defined according to [48] $\langle \hat{\psi}^\dagger(x)\hat{\psi}(x') \rangle = \sqrt{\rho(x)\rho(x')} \exp[-\frac{1}{2}(\delta\hat{\phi}_{xx'})^2]$, where $\delta\hat{\phi}_{xx'} = \hat{\phi}(x) - \hat{\phi}(x')$ is the phase difference operator and $\rho(x) = \langle \hat{\psi}^\dagger(x)\hat{\psi}(x) \rangle$ is the mean local density.

The correlation dip is due to the presence and geometry of the trap and, consequently, related to the shape of the occupied orbitals and exists even for relatively small interaction couplings. The built-in self-consistency of the MCTDH method is crucial in order to correctly describe the correlation phenomena in trapped quantum many-body systems, because the depth and location of the correlation dip sensitively depends on the self-consistently determined orbital shape.

We note in the top panel of Fig. 2 a sizable quantitative difference to the analytical solutions already for interaction strengths that are far below the hard-core limit of $g \rightarrow \infty$. However, for couplings commonly realized in experiments with magnetic traps (see for concrete estimates

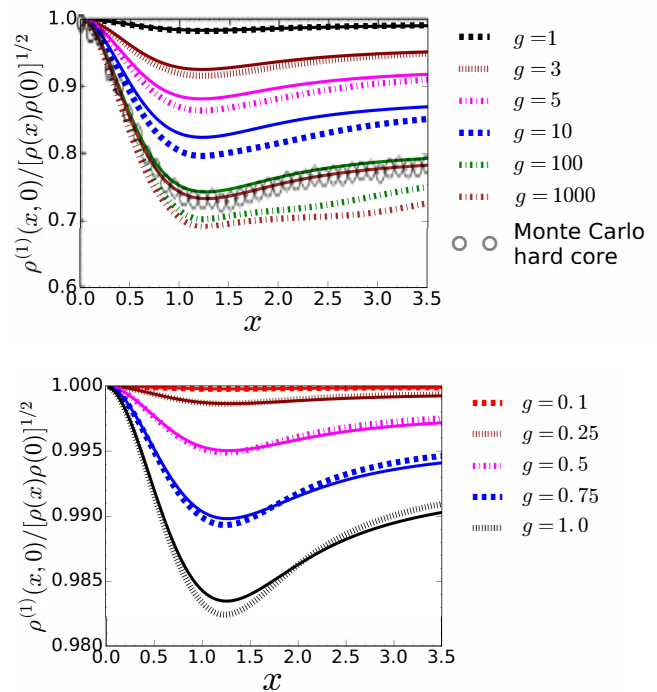


FIG. 2. Top: Single-particle density matrix $\rho^{(1)}(x, x')/\sqrt{\rho(x)\rho(x')}$ as a function of x and $x' = 0$ for $N = 2$ interacting bosons in a harmonic trap, in the strong coupling regime. The gray circles are the Monte Carlo results of Minguzzi *et al.* [34] for hard-core bosons ($g \rightarrow \infty$), with the size of the circles representing the error bars in the Monte Carlo data. The lines are MCTDH results for various g and $M = 10$. The solid lines show the analytical result. Bottom: Comparison of MCTDH results ($M = 10$) with the 1D analytical solution in the range of intermediate interaction couplings.

below), the agreement between the analytical results and MCTDH is very satisfactory, see the lower panel of Fig. 2, even for the relatively modest number of orbitals $M = 10$ used in these calculations. The characteristic dip in the correlation function appears for any interaction strength and is correctly reproduced by the MCTDH method to good accuracy in its location, while the depth of the dip is somewhat exaggerated by MCTDH in particular for larger than intermediate couplings, $g \gg 1$.

Fragmentation. Using the single-particle density matrix, one may formally define an important figure of merit, the fragmentation. By diagonalizing the single-particle density matrix, one obtains its eigenfunctions, ϕ_i , and eigenvalues, N_i , which are in the many-body context referred to as *natural orbitals* and *occupation numbers*, respectively,

$$\rho^{(1)}(x, x') = \sum_{i=0}^{M-1} N_i \phi_i^*(x') \phi_i(x). \quad (8)$$

Here, the sum for MCTDH runs over the finite set

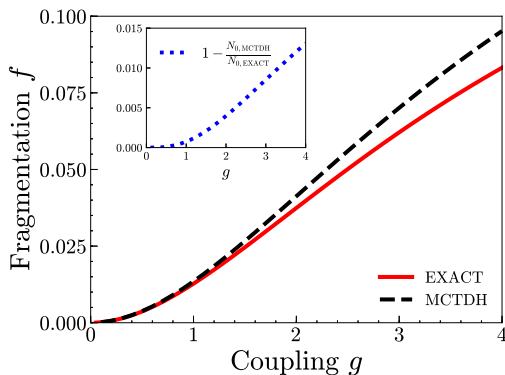


FIG. 3. Fragmentation f as defined in Eq. (9), obtained from the diagonalization of the analytical single-particle density matrix (red solid) and from MCTDH (black dashed) with $M = 10$ orbitals, for the range $g = 0.1, \dots, 4$. The inset shows the relative numerical error in the occupation number of the energetically lowest orbital.

$i = \{0, \dots, M - 1\}$ and for the exact solution over an infinite set $i = \{0, \dots, \infty\}$. While a “macroscopic” orbital occupation defining fragmented condensates [49, 50] obviously cannot be obtained when $N = 2$, the average relative occupation of orbitals other than the energetically lowest is still well defined. We thus *define* the

$$\text{Fragmentation} \quad f := \frac{N - N_0}{N} \quad (9)$$

as the relative occupation number of all orbitals excluding the most populated one (which has $i := 0$), sorting occupation numbers N_i from largest to smallest.

In Fig. 3, we display the exact fragmentation f calculated using the exact density matrix in Eq. (6). We obtain the exact occupation numbers by first expressing $\rho^{(1)}(x, x')$ in a harmonic oscillator eigenfunctions basis of dimension $M_{\text{ho}} = 50$ (which proved sufficiently large) and by then diagonalizing it, evaluating the integrals via the Gauss-Hermite approximation. The sizable difference when $g \gg 1$, is further illustrated in the inset, which shows the error in the occupation of the lowest orbital, $1 - N_{0,\text{MCTDH}}/N_{0,\text{exact}}$. Note that the fragmentation f obtained via MCTDH is always *larger* than the exact value, which is in agreement with the observation that the former approach overestimates the correlation dip in the first-order correlations (and hence also overestimates phase fluctuations), cf. Fig. 2.

Natural orbitals. In Fig. 4, we plot the first six natural orbitals contained in the diagonalized single-particle density matrix Eq. (8). We conclude that sizable deviations between exact and MCTDH natural orbitals start to occur for $i = 4$ and above; within the resolution of the figure, we detected no discernible deviation in the first four, that is energetically lowest, natural orbitals, $i = 0, \dots, 3$, the exact and MCTDH curves lying precisely on top of

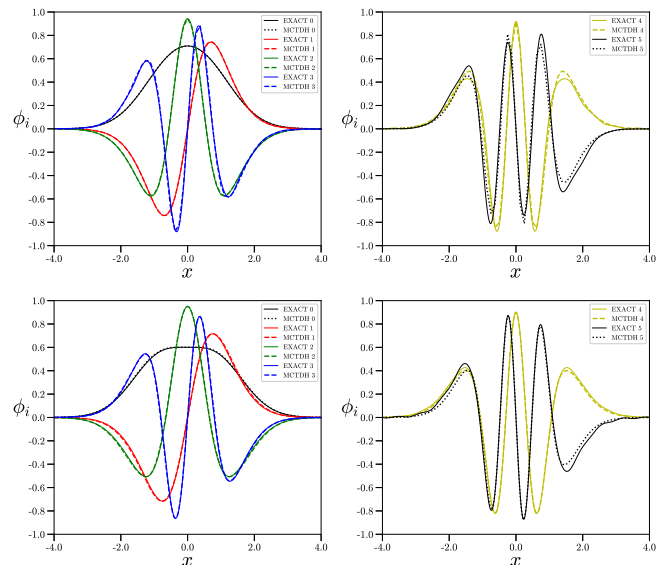


FIG. 4. The first six natural orbitals $\phi_i(x)$, $i = 0, \dots, 5$, in Eq. (8), obtained via MCTDH (dashed, $M = 10$) and the exact results (solid), from diagonalizing the single-particle density matrix in Eq. (6) (solid). Left: $i = 0, \dots, 3$, right: $i = 4, 5$. Top row: $g = 1$, bottom row $g = 10$.

each other in this range. We also note in this context that the occupation numbers N_i for $i > 2$ are very small. For example, N_3 is about an order of magnitude less than N_2 , for both $g = 1$ and $g = 10$ and for both MCTDH and exact occupation numbers [51]. Therefore, it is indeed the occupation number difference of the lower natural orbitals (rather than their precise shape) which explains the different fragmentation obtained by MCTDH and exact solution. As a corollary, going to much larger M does not significantly decrease the f -difference further.

Conclusion. We now illustrate the above general considerations by concrete numbers for an experimentally realizable system. In a *quasi-1D* Bose gas, and far away from geometric resonances [52], we have $g = 4a_{\text{sc}}l/l_{\perp}^2$ where l_{\perp} is the transverse trapping length. For ^{87}Rb , this implies $g = 1.96 \times a_{\text{sc}}[a_{\text{Rb}}]\nu_{\perp}[\text{kHz}]/\sqrt{\nu[\text{Hz}]}$, where the background scattering length $a_{\text{Rb}} = 5.29$ nm, $\omega_{\perp,\nu} = 2\pi\nu_{\perp,\nu}$, and the frequencies are scaled with typical experimental values see, e.g., [53, 54]. With the background scattering length of ^{87}Rb , and $g \sim \mathcal{O}(1)$, the MCTDH results are in satisfactory accord with the analytical result for quasi-1D setups accessible by magnetic trapping.

Limits of the MCTDH approach can be explored, e.g., in optical lattices when one increases g towards the Tonks-Girardeau regime [36, 37]. While only at a filling of two per one-dimensional tube our results can strictly be applied, we anticipate that also for larger N qualitatively similar features as those in Fig. 2, and in particular the trap-induced correlation dip, should persist and be observable for example with (a combination of) Feshbach

resonances [42] and higher aspect ratios. Variation of g and N and measurement of, e.g., the first-order correlations which have been investigated here paves the way for a quantitative experimental assessment of the accuracy of MCTDH. The detailed analysis of higher-order correlations [55] will then reveal further precise information on the applicability of the MCTDH method to strongly correlated systems.

Acknowledgments. This research was supported by the NRF Korea, Grant Nos. 2014R1A2A2A01006535 and 2017R1A2A2A05001422. OVM acknowledges support by Grant No. 2015616 of the Binational USA-Israel Science Foundation.

-
- [1] H.-D. Meyer, U. Manthe, and L. S. Cederbaum, “The multi-configurational time-dependent Hartree approach,” *Chemical Physics Letters* **165**, 73–78 (1990).
- [2] H.-D. Meyer, F. Gatti, and G. A. Worth, eds., *Multi-dimensional Quantum Dynamics: MCTDH Theory and Applications* (John Wiley & Sons, 2009).
- [3] Ofir E. Alon, Alexej I. Streltsov, and Lorenz S. Cederbaum, “Multi-configurational time-dependent Hartree method for bosons: Many-body dynamics of bosonic systems,” *Phys. Rev. A* **77**, 033613 (2008).
- [4] A. U. J. Lode, M. Tsatsos, and E. Fasshauer, “MCTDH-X: The time-dependent multiconfigurational Hartree for indistinguishable particles software,” <http://ultracold.org>.
- [5] M. H. Beck, A. Jäckle, G. A. Worth, and H.-D. Meyer, “The multiconfiguration time-dependent Hartree (MCTDH) method: a highly efficient algorithm for propagating wavepackets,” *Physics Reports* **324**, 1–105 (2000).
- [6] Axel U. J. Lode, Kaspar Sakmann, Ofir E. Alon, Lorenz S. Cederbaum, and Alexej I. Streltsov, “Numerically exact quantum dynamics of bosons with time-dependent interactions of harmonic type,” *Phys. Rev. A* **86**, 063606 (2012).
- [7] Julian Grond, Alexej I. Streltsov, Axel U. J. Lode, Kaspar Sakmann, Lorenz S. Cederbaum, and Ofir E. Alon, “Excitation spectra of many-body systems by linear response: General theory and applications to trapped condensates,” *Phys. Rev. A* **88**, 023606 (2013).
- [8] Alexej I. Streltsov, “Quantum systems of ultracold bosons with customized interparticle interactions,” *Phys. Rev. A* **88**, 041602 (2013).
- [9] Uwe R. Fischer, Axel U. J. Lode, and Budhaditya Chatterjee, “Condensate fragmentation as a sensitive measure of the quantum many-body behavior of bosons with long-range interactions,” *Phys. Rev. A* **91**, 063621 (2015).
- [10] Sven Krönke and Peter Schmelcher, “Two-body correlations and natural-orbital tomography in ultracold bosonic systems of definite parity,” *Phys. Rev. A* **92**, 023631 (2015).
- [11] Sven Krönke and Peter Schmelcher, “Born-Bogoliubov-Green-Kirkwood-Yvon hierarchy for ultracold bosonic systems,” *Phys. Rev. A* **98**, 013629 (2018).
- [12] Shachar Klaiman and Ofir E. Alon, “Variance as a sensitive probe of correlations,” *Phys. Rev. A* **91**, 063613 (2015).
- [13] Shachar Klaiman and Lorenz S. Cederbaum, “Overlap of exact and Gross-Pitaevskii wave functions in Bose-Einstein condensates of dilute gases,” *Phys. Rev. A* **94**, 063648 (2016).
- [14] Kaspar Sakmann and Mark Kasevich, “Single-shot simulations of dynamic quantum many-body systems,” *Nature Physics* **12**, 451–454 (2016).
- [15] Axel U. J. Lode and Christoph Bruder, “Fragmented Superradiance of a Bose-Einstein Condensate in an Optical Cavity,” *Phys. Rev. Lett.* **118**, 013603 (2017).
- [16] M. C. Tsatsos, J. H. V. Nguyen, A. U. J. Lode, G. D. Telles, D. Luo, V. S. Bagnato, and R. G. Hulet, “Granulation in an atomic Bose-Einstein condensate,” arXiv:1707.04055 [cond-mat.quant-gas].
- [17] K. Sakmann and J. Schmiedmayer, “Conservation of angular momentum in Bose-Einstein condensates requires many-body theory,” arXiv:1802.03746 [cond-mat.quant-gas].
- [18] P. D. Drummond and J. Brand, “Comment on: ‘Single-shot simulations of dynamic quantum many-body systems’,” arXiv:1610.07633 [cond-mat.quant-gas].
- [19] K. Sakmann and M. Kasevich, “Reply to the correspondence of Drummond and Brand [arXiv:1610.07633],” arXiv:1702.01211 [cond-mat.quant-gas].
- [20] M. K. Olsen, J. F. Corney, R. J. Lewis-Swan, and A. S. Bradley, “Correspondence on ‘Single-shot simulations of dynamic quantum many-body systems’,” arXiv:1702.00282 [quant-ph].
- [21] Jayson G. Cosme, Christoph Weiss, and Joachim Brand, “Center-of-mass motion as a sensitive convergence test for variational multimode quantum dynamics,” *Phys. Rev. A* **94**, 043603 (2016).
- [22] Kang-Soo Lee and Uwe R. Fischer, “Truncated many-body dynamics of interacting bosons: A variational principle with error monitoring,” *International Journal of Modern Physics B* **28**, 1550021 (2014).
- [23] Uwe Manthe, “The multi-configurational time-dependent Hartree approach revisited,” *The Journal of Chemical Physics* **142**, 244109 (2015).
- [24] Benedikt Kloss, Irene Burghardt, and Christian Lubich, “Implementation of a novel projector-splitting integrator for the multi-configurational time-dependent Hartree approach,” *The Journal of Chemical Physics* **146**, 174107 (2017).
- [25] Hans-Dieter Meyer and Haobin Wang, “On regularizing the MCTDH equations of motion,” *The Journal of Chemical Physics* **148**, 124105 (2018).
- [26] Peter D. Drummond and Bogdan Opanchuk, “Truncated Wigner dynamics and conservation laws,” *Phys. Rev. A* **96**, 043616 (2017).
- [27] Y. Castin and R. Dum, “Low-temperature Bose-Einstein condensates in time-dependent traps: Beyond the $U(1)$ symmetry-breaking approach,” *Phys. Rev. A* **57**, 3008–3021 (1998).
- [28] Lorenz S. Cederbaum, “Exact many-body wave function and properties of trapped bosons in the infinite-particle limit,” *Phys. Rev. A* **96**, 013615 (2017).
- [29] Elliott H. Lieb and Robert Seiringer, “Proof of Bose-Einstein Condensation for Dilute Trapped Gases,” *Phys. Rev. Lett.* **88**, 170409 (2002).
- [30] Elliott H. Lieb, Robert Seiringer, and Jakob Yngvason, “One-Dimensional Bosons in Three-Dimensional Traps,” *Phys. Rev. Lett.* **91**, 150401 (2003).

- [31] Thomas Busch, Berthold-Georg Englert, Kazimierz Rzazewski, and Martin Wilkens, “Two Cold Atoms in a Harmonic Trap,” *Foundations of Physics* **28**, 549–559 (1998).
- [32] Zbigniew Idziaszek and Tommaso Calarco, “Analytical solutions for the dynamics of two trapped interacting ultracold atoms,” *Phys. Rev. A* **74**, 022712 (2006).
- [33] See supplemental material for concise summaries of the derivation of the 1D analytical solution and of the MCTDH method.
- [34] A. Minguzzi, P. Vignolo, and M. P. Tosi, “High-momentum tail in the Tonks gas under harmonic confinement,” *Physics Letters A* **294**, 222–226 (2002).
- [35] M. A. Cazalilla, R. Citro, T. Giamarchi, E. Orignac, and M. Rigol, “One dimensional Bosons: From Condensed Matter Systems to Ultracold Gases,” *Rev. Mod. Phys.* **83**, 1405–1466 (2011).
- [36] Belén Paredes, Artur Widera, Valentin Murg, Olaf Mandel, Simon Fölling, Ignacio Cirac, Gora V Shlyapnikov, Theodor W Hänsch, and Immanuel Bloch, “Tonks-Girardeau gas of ultracold atoms in an optical lattice.” *Nature* **429**, 277 (2004).
- [37] Toshiya Kinoshita, Trevor Wenger, and David S Weiss, “Observation of a one-dimensional Tonks-Girardeau gas,” *Science* **305**, 1125 (2004).
- [38] Elliott H. Lieb and Werner Liniger, “Exact Analysis of an Interacting Bose Gas. I. The General Solution and the Ground State,” *Phys. Rev.* **130**, 1605–1616 (1963).
- [39] Kaspar Sakmann, Alexej I. Streltsov, Ofir E. Alon, and Lorenz S. Cederbaum, “Exact Quantum Dynamics of a Bosonic Josephson Junction,” *Phys. Rev. Lett.* **103**, 220601 (2009).
- [40] An exactly solvable model (which is readily integrable for any N) and the convergence of MCTDH towards its solutions was studied with a harmonic interaction potential in Ref. [6], however with the obvious limitation that this interaction is not the experimentally realized one.
- [41] We note that MCTDH has previously been applied to the 1D $N = 2$ contact interaction problem for *anharmonic* potentials, however without an attempt to connect the results to the exactly known harmonic potential solution. See Christian Matthies, Sascha Zöllner, Hans-Dieter Meyer, and Peter Schmelcher, “Quantum dynamics of two bosons in an anharmonic trap: Collective versus internal excitations,” *Phys. Rev. A* **76**, 023602 (2007).
- [42] Cheng Chin, Rudolf Grimm, Paul Julienne, and Eite Tiesinga, “Feshbach resonances in ultracold gases,” *Reviews of Modern Physics* **82**, 1225–1286 (2010).
- [43] M. Abramowitz and I. A. Stegun, *Handbook of mathematical functions* (Dover Publications, New York, 1970).
- [44] Axel U. J. Lode, “Multiconfigurational time-dependent Hartree method for bosons with internal degrees of freedom: Theory and composite fragmentation of multicomponent Bose-Einstein condensates,” *Phys. Rev. A* **93**, 063601 (2016).
- [45] Elke Fasshauer and Axel U. J. Lode, “Multiconfigurational time-dependent Hartree method for fermions: Implementation, exactness, and few-fermion tunneling to open space,” *Phys. Rev. A* **93**, 033635 (2016).
- [46] Shachar Klaiman, Raphael Beinke, Lorenz S. Cederbaum, Alexej I. Streltsov, and Ofir E. Alon, “Variance of an anisotropic Bose-Einstein condensate,” *Chemical Physics* **509**, 45–54 (2018).
- [47] We note the curious historical fact that [34] was apparently not aware of [31], which appeared four years earlier.
- [48] O. V. Marchukov and U. R. Fischer, “Fragmentation of phase-fluctuating condensates,” arXiv:1701.06821 [cond-mat.quant-gas].
- [49] Oliver Penrose and Lars Onsager, “Bose-Einstein Condensation and Liquid Helium,” *Phys. Rev.* **104**, 576–584 (1956).
- [50] Anthony J. Leggett, “Bose-Einstein condensation in the alkali gases: Some fundamental concepts,” *Rev. Mod. Phys.* **73**, 307–356 (2001).
- [51] Specifically, for $g = 1$, $N_2 \simeq 2.09 \times 10^{-3}$ (exact), $N_2 \simeq 2.20 \times 10^{-4}$ (MCTDH, $M = 10$), $N_2 \simeq 2.14 \times 10^{-3}$ (MCTDH, $M = 33$), while $N_3 \simeq 4.12 \times 10^{-4}$ (exact), $N_3 \simeq 4.34 \times 10^{-4}$ (MCTDH, $M = 10$), $N_3 \simeq 4.27 \times 10^{-3}$ (MCTDH, $M = 33$).
- [52] Maxim Olshanii, “Atomic Scattering in the Presence of an External Confinement and a Gas of Impenetrable Bosons,” *Phys. Rev. Lett.* **81**, 938 (1998).
- [53] T. Betz, S. Manz, R. Bücker, T. Berrada, Ch. Koller, G. Kazakov, I. E. Mazets, H.-P. Stimming, A. Perrin, T. Schumm, and J. Schmiedmayer, “Two-Point Phase Correlations of a One-Dimensional Bosonic Josephson Junction,” *Phys. Rev. Lett.* **106**, 020407 (2011).
- [54] Bess Fang, Aisling Johnson, Tommaso Roscilde, and Isabelle Bouchoule, “Momentum-Space Correlations of a One-Dimensional Bose Gas,” *Phys. Rev. Lett.* **116**, 050402 (2016).
- [55] Thomas Schweigler, Valentin Kasper, Sebastian Erne, Igor Mazets, Bernhard Rauer, Federica Cataldini, Tim Langen, Thomas Gasenzer, Jürgen Berges, and Jörg Schmiedmayer, “Experimental characterization of a quantum many-body system via higher-order correlations,” *Nature* **545**, 323–326 (2017).

Supplemental Material

EXACT SOLUTION FOR TWO CONTACT-INTERACTING PARTICLES IN A ONE-DIMENSIONAL HARMONIC TRAP

We delineate here a compact derivation of the one-dimensional (1D) variant of the analytical, closed form solution of Busch et al. in 3D [31], cf. its extension to anisotropic traps in [32]. The calculations for the 1D case follow the same logic as for the 3D case of Ref. [31]. The Hamiltonian of the problem is given by Eq. (1) in the main text and we scale lengths and energies by $\sqrt{\hbar/m\omega}$ and $\hbar\omega$, respectively. To separate the center of mass (COM) and relative motion of the atoms in the system, we substitute $r = \frac{1}{\sqrt{2}}(x_1 - x_2)$ and $R = \frac{1}{\sqrt{2}}(x_1 + x_2)$, for the relative and COM coordinates, respectively. In accordance with the Ref. [31], the ‘‘unconventional’’ $\sqrt{2}$ factors in the definitions are in order for the effective masses of COM and relative motions to be identical. Then the Hamiltonian (1) becomes

$$H = H_{\text{COM}} + H_{\text{rel}}, \quad (\text{S1})$$

with $H_{\text{COM}} = -\frac{1}{2}\frac{\partial^2}{\partial R^2} + \frac{1}{2}R^2$ and $H_{\text{rel}} = -\frac{1}{2}\frac{\partial^2}{\partial r^2} + \frac{1}{2}r^2 + g\delta(r)$. The Schrödinger equation reads $H\Psi(x_1, x_2) = E\Psi(x_1, x_2)$, where E is the dimensionless energy eigenvalue of the Hamiltonian in Eq. (S1). The wavefunction of the system can be written as a product, $\Psi(x_1, x_2) = \Psi_{\text{COM}}(R)\psi_{\text{rel}}(r)$.

The COM wavefunction can be written as the one for a harmonic oscillator $\Psi_{\text{COM}} = \frac{1}{\sqrt{2^n n!}} \frac{1}{\pi^{1/4}} e^{-R^2/2} H_n(R)$, where H_n are the n^{th} order Hermite polynomials. By separation of variables, the Schrödinger equation for the relative motion reads

$$-\frac{1}{2}\frac{\partial^2}{\partial r^2}\psi_{\text{rel}} + \frac{1}{2}r^2\psi_{\text{rel}} + \frac{g}{\sqrt{2}}\delta(r)\psi_{\text{rel}} = \varepsilon\psi_{\text{rel}}, \quad (\text{S2})$$

with $\varepsilon = E - (n + \frac{1}{2})$.

In order to solve Eq. (S2) we can expand the relative motion wavefunction in a basis of harmonic oscillator eigenfunctions, $\phi_k(r) = \frac{1}{\sqrt{2^k k!}} \frac{1}{\pi^{1/4}} e^{-r^2/2} H_k(r)$. Thus,

$$\psi_{\text{rel}}(r) = \sum_{k=0}^{\infty} C_k \phi_k(r). \quad (\text{S3})$$

Then, the Schrödinger Eq. (S2) becomes

$$\sum_{k=0}^{\infty} \left(k + \frac{1}{2}\right) C_k \phi_k(r) + \frac{1}{\sqrt{2}} g \delta(r) \sum_{k=0}^{\infty} C_k \phi_k(r) = \varepsilon \sum_{k=0}^{\infty} C_k \phi_k(r). \quad (\text{S4})$$

Multiplying Eq. (S4) by $\phi_m(r)$, integrating over space, we can find the coefficients $C_k = \frac{A\phi_k(0)}{k + \frac{1}{2} - \varepsilon}$, where $A = -\frac{g}{\sqrt{2}} \left(\sum_{i=0}^{\infty} C_i \phi_i(r) \right)_{r \rightarrow 0}$ is a constant that does not depend on the index k .

Inserting C_k back into Eq. (S4) we obtain

$$\left(\sum_{k=0}^{\infty} \frac{\phi_k(0)\phi_k(r)}{k + \frac{1}{2} - \varepsilon} \right)_{r \rightarrow 0} = -\frac{\sqrt{2}}{g}. \quad (\text{S5})$$

Using the properties of the Hermite polynomials, it is clear that $\phi_k(0)$ and the whole left hand side of Eq. (S5) is nonzero only for even values of $k = 2l$. Then, using the relation between Hermite and Laguerre polynomials [43], $H_{2n}(x) = (-1)^n 2^{2n} n! L_n^{(-1/2)}(x^2)$, Eq. (S5) reads

$$\left(\sum_{l=0}^{\infty} \frac{e^{-r^2/2} L_l^{(-1/2)}(r^2)}{l - \nu} \right)_{r \rightarrow 0} = -\frac{2\sqrt{2}}{g}, \quad (\text{S6})$$

where we have introduced a new quantum number, $\nu = \frac{\varepsilon}{2} - \frac{1}{4}$. Now we recall the generating function for Laguerre

polynomials [43] $\sum_{l=0}^{\infty} z^l L_l^{(-1/2)}(x^2) = \frac{1}{(1-z)^{1/2}} e^{-\frac{zx^2}{1-z}}$, and, by employing the integral representation $(l-\nu)^{-1} = \int_0^{\infty} \frac{dy}{(1+y)^2} \left(\frac{y}{1+y}\right)^{l-\nu-1}$, the left hand side of Eq. (S6) yields

$$\left(\sum_{l=0}^{\infty} \frac{e^{-r^2/2} L_l^{(-1/2)}(r^2)}{l-\nu} \right)_{r \rightarrow 0} = \left(e^{-r^2/2} \Gamma(-\nu) U(-\nu; \frac{1}{2}; r^2) \right)_{r \rightarrow 0}, \quad (\text{S7})$$

where $U(a, b; z)$ is a confluent hypergeometric function and we used the relation $\Gamma(a)U(a, b; z) = \int_0^{\infty} e^{-zt} t^{a-1} (1+t)^{b-a-1} dt$ [43].

Note that upon employing the known property of the confluent hypergeometric function at $x = 0$, $U(-\nu, \frac{1}{2}; x^2 = 0) \approx \frac{\sqrt{\pi}}{\Gamma(-\nu + \frac{1}{2})}$ the Eq. (S5) takes the simple form

$$\frac{\Gamma(-\nu + \frac{1}{2})}{\Gamma(-\nu)} = -\frac{g}{2\sqrt{2}}, \quad (\text{S8})$$

from which we can find the dimensionless energy, $\varepsilon = 2\nu + \frac{1}{2}$. The relative wavefunction reads

$$\psi_{\text{rel}} = -\text{const.} \times e^{-r^2/2} U(-\nu, \frac{1}{2}; r^2), \quad (\text{S9})$$

where the constant can be found using normalization.

THE MCTDH METHOD

A system of N interacting bosons is generally described by the time-dependent Schrödinger equation for $\Psi = \Psi(x_1, \dots, x_N; t)$

$$\left[\sum_{i=1}^N \hat{h}(x_i; t) + \sum_{i>j}^N \hat{W}(x_i - x_j) \right] \Psi = i\hbar \frac{\partial \Psi}{\partial t}, \quad (\text{S10})$$

where $\hat{h}(x_i; t) = \frac{p_i^2}{2m} + V(x_i)$ is the single-particle Hamiltonian, x_i and p_i are position and momentum operators of a given boson i , and $V(x_i)$ is the potential energy. The term $\hat{W}(x_i - x_j)$ is the pairwise particle interaction operator. The many-body wavefunction, $\Psi(x_1, \dots, x_N; t)$, in the MCTDH formulation is expressed by the following ansatz

$$|\Psi\rangle = \sum_{\{\vec{N}\}} C_{\vec{N}}(t) |\vec{N}; t\rangle, \quad (\text{S11})$$

where the basis of (time dependent) *permanents* $|\vec{N}; t\rangle = \frac{1}{\sqrt{N_0! N_1! \dots N_{M-1}!}} (b_0^\dagger(t))^{N_0} (b_1^\dagger(t))^{N_1} \dots (b_{M-1}^\dagger(t))^{N_{M-1}} |\text{vac}\rangle$ consists of all possible symmetrized wavefunction products of N particles distributed over M single-particle functions (*orbitals*), where $\vec{N} = (N_0, N_1, \dots, N_{M-1})$ and $\sum_{i=0}^{M-1} N_i = N$, i.e. N_j represents the occupation of the orbital j , and $C_{\vec{N}}(t)$ are the time-dependent expansion coefficients. Clearly, the ansatz (S11) is exact if $M \rightarrow \infty$, that is if we consider the full, untruncated Fock space of the many-particle system. Note that for $N = 2$, the basis size is relatively moderate and equals $\frac{1}{2}(M+1)!/(M-1)!$.

The Dirac-Frenkel variational procedure applied to the action $S[\{C_{\vec{N}}(t)\}, \{\varphi_j(x_i; t)\}] = \int dt [\langle \Psi | \hat{H} - i\hbar \frac{\partial}{\partial t} | \Psi \rangle - \sum_{j,k=1}^M \mu_{jk}(t) (\langle \varphi_j | \varphi_k \rangle - \delta_{jk})]$, where $\mu_{jk}(t)$ are time-dependent Lagrange multipliers, ensuring that the orbitals remain orthonormal, gives the equations of motion

$$\begin{aligned} i\hbar \frac{\partial \mathbf{C}(t)}{\partial t} &= \mathbf{H}(t) \mathbf{C}(t), \\ i\hbar \frac{\partial |\varphi_j\rangle}{\partial t} &= \hat{P} \left[\hat{h} |\varphi_j\rangle + \sum_{k,s,q,l=1}^M \rho_{jk}^{-1} \rho_{ksql} \hat{W}_{sl} |\varphi_q\rangle \right]. \end{aligned} \quad (\text{S12})$$

Here, $\mathbf{C}(t)$ is the column vector that consists of all possible expansion coefficients $C_{\vec{N}}(t)$, $\mathbf{H}(t)$ corresponds to the time-dependent Hamiltonian matrix in the corresponding basis $|\vec{N}; t\rangle$, $\hat{W}_{sl} = \int \int dx dx' \varphi_s^*(x) W(x - x') \varphi_l(x')$ are the local interaction potentials, $\hat{P} = 1 - \sum_{k'=1}^M |\varphi_{k'}\rangle \langle \varphi_{k'}|$ is a projection operator onto the subspace orthogonal to the one spanned by orbitals $\varphi_{k'}$, and ρ_{jk} and ρ_{ksql} are the matrix elements of the single-particle and two-particle density matrices, respectively.
